Perovskite Stability

Deutsche Ausgabe: DOI: 10.1002/ange.201602236
Internationale Ausgabe: DOI: 10.1002/anie.201602236

Organolead Halide Perovskite Nanocrystals: Branched Capping Ligands Control Crystal Size and Stability

Binbin Luo, Ying-Chih Pu, Sarah A. Lindley, Yi Yang, Liqiang Lu, Yat Li, Xueming Li, and Jin Z. Zhang**

Abstract: *$CH_3NH_3PbBr_3$ perovskite nanocrystals (PNCs) of different sizes (ca. 2.5–100 nm) with high photoluminescence (PL) quantum yield (QY; ca. 15–55 %) and product yield have been synthesized using the branched molecules, APTES and NH_2-POSS, as capping ligands. These ligands are sterically hindered, resulting in a uniform size of PNCs. The different capping effects resulting from branched versus straight-chain capping ligands were compared and a possible mechanism proposed to explain the dissolution–precipitation process, which affects the growth and aggregation of PNCs, and thereby their overall stability. Unlike conventional PNCs capped with straight-chain ligands, APTES-capped PNCs show high stability in protic solvents as a result of the strong steric hindrance and propensity for hydrolysis of APTES, which prevent such molecules from reaching and reacting with the core of PNCs.*

Organolead halide perovskites, a class of materials with the typical formula $APbX_3$ ($A = Cs^+$ or $CH_3NH_3^+$; X = I, Br, Cl), have emerged as promising materials for photovoltaics (PV),[1] light-emitting diodes (LED),[2] photodetectors,[3] and lasers.[4] Yet, their practical applications are hindered by their instability, which depends on factors such as oxygen, UV light, temperature, moisture, and surface defects.[5] Therefore, it is urgent to understand the degradation mechanism and find solutions to address this issue. Compared to bulk materials, nanocrystals (NCs) are often less stable because of their large surface-to-volume (S/V) ratio and high percentage of surface atoms with dangling bonds, making them a good model system for studying material instability.

PNCs have been used for LED applications because of their high PL QY (ca. 90 %), narrow emission bands (ca. 20 nm), and tunable emission spanning the whole visible range.[2a–c,6] As a consequence of the high density of trap states that often result in non-radiative recombination, it is necessary to passivate the surface of PNCs using appropriate capping ligands to achieve high PL QY.[2b,7] Moreover, simulation studies have shown that surface defects may increase degradation of PNCs.[8] Therefore, proper passivation is also important for improving the stability of PNCs. With this in mind, straight-chain octylammonium bromide (OABr) and octadecylammonium bromide (ODABr) were used as capping ligands for synthesizing PNCs.[5a] However, the relatively weak passivation ability of these ligands resulted in low PL QY (ca. 20 %) and non-uniform products, including perovskite nanoparticles (PNPs) and perovskite nanosheets (PNSs).[5a,9] Zhang et al. successfully synthesized perovskite quantum dots (PQDs) with high PL QY (ca. 70 %), when octylamine (OA) was used as the capping ligand.[2b] Nevertheless, the product yield of PQDs with high PL QY is low due to the formation of large perovskite particles during the precipitation step.[6] Although both OA and OABr can serve as capping ligands, uniform particles with a single emission band and high PL QY remain elusive with these materials. More importantly, the PNCs capped by these ligands show poor stability in polar and protic solvents, which hinders further functionalization and sensitization since many reactions are conducted in polar and protic solvents.

Herein, we describe branched capping ligands, (3-aminopropyl)triethoxysilane (APTES) and polyhedral oligomeric silsesquioxane (POSS) PSS-[3-(2-aminoethyl)amino]propyl-heptaisobutyl substituted (NH_2-POSS; Figure 1 a), and their successful implementation as passivators and stabilizers of PNCs. By adjusting the amount of the capping ligands, uniform PNCs with high PL QY (ca. 15–55 %), tunable size (ca. 2.5–100 nm), and emission (452–524 nm) could be synthesized in a controlled fashion. Moreover, the stability of APTES-capped PNCs of different sizes was studied in protic solvents; decomposition by solvent was impeded because of the strong steric hindrance and hydrolysis properties of APTES.

PNC_{OA}, $PNC_{NH2\text{-}POSS}$, and PNC_{APTES} samples were synthesized using a dissolution–precipitation method, as shown in Figure 1 b. *N*,*N*-dimethylformamide (DMF, 1 mL) precursor solution was injected into toluene (10 mL) to precipitate PNCs. The PNC supernatant and precipitate were obtained by centrifuging the resultant solution at 13000 rpm min^{-1} for 6 minutes. The PNC solution was prepared by injecting DMF (4 μL) precursor solution into toluene (4 mL) without any further purification, and underwent optical characterization directly. Transmission electron microscopy (TEM) and high resolution TEM (HRTEM) were

[*] B. Luo, S. A. Lindley, Y. Yang, L. Lu, Prof. Y. Li, Prof. J. Z. Zhang
Department of Chemistry and Biochemistry, University of California Santa Cruz, CA 95064 (USA)
E-mail: zhang@ucsc.edu
B. Luo, Prof. X. Li
Department of Chemistry and Chemical Engineering
Chongqing University, Chongqing, 400044 (China)
E-mail: xuemingli@cqu.edu.cn
L. Lu
Faculty of Materials Science and Chemistry
China University of Geosciences, Wuhan, 430074 (China)
Prof. Y.-C. Pu
Department of Materials Science, National University of Tainan
Tainan, 70005 (Taiwan, Republic of China)

Supporting information for this article can be found under: http://dx.doi.org/10.1002/anie.201602236.

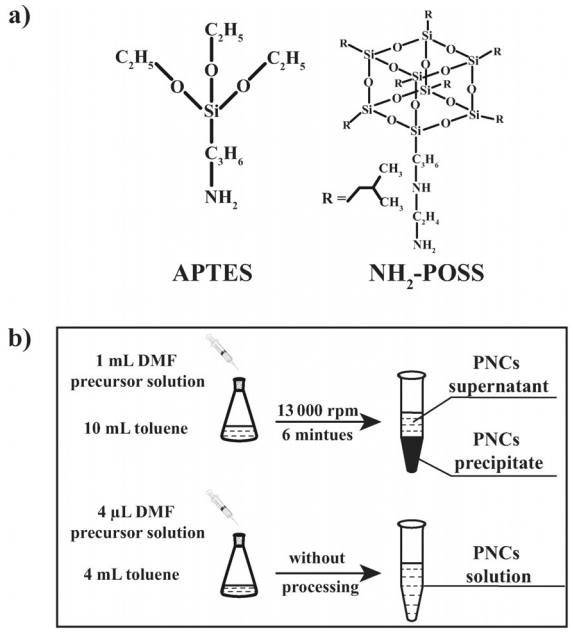

Figure 1. a) Molecular structure of APTES and NH_2-POSS, b) Synthetic procedure for PNCs.

used to characterize the morphology of PNC_{APTES} (Figure 2). For PNC_{APTES} precipitates prepared with low concentrations of APTES, $PNC_{APTES\text{-}2}$ (Figure 2a) and $PNC_{APTES\text{-}4}$ (Figure 2b), cubic nanoparticles with an average length of about 100 and 80 nm were obtained, respectively. After increasing the APTES concentration to 8 μL mL^{-1}, smaller PNCs with a mean diameter of 7.8 ± 1.6 nm were obtained, attributed to the coordinating effect of capping ligands, which resulted in a slower delivery rate of monomer.[10] With a further increase in APTES concentration, more uniform and monodisperse PNCs with an average diameter of 5.1 ± 0.6 nm, 3.1 ± 0.4 nm, and 2.5 ± 0.4 nm were obtained, labeled as $PNC_{APTES\text{-}16}$, $PNC_{APTES\text{-}32}$, and $PNC_{APTES\text{-}64}$. No PNSs were found in the samples when the concentration of APTES was > 8 μL mL^{-1}, because the strong steric hindrance of branched APTES resulted in spherical particles. In contrast, the products included a combination of spherical, sheet-like, and belt-like PNCs when straight capping ligands, OA and OABr, were used in the synthesis of PNCs (Supporting Information, Figure S1), indicating the ability of branched APTES to control the uniformity of PNCs. HRTEM images of a single PNC show lattice spacing of 2.6 and 3.0 Å, which could be assigned to the (0 2 1) and (0 0 2) planes of cubic $CH_3NH_3PbBr_3$.[5a] The broader XRD peaks (Supporting Information, Figure S2a) also indicate the formation of smaller PNCs with increasing APTES concentration. An FTIR spectrum of the PNC (Supporting Information, Figure S2b) shows a broad O–H asymmetric stretching band from 3300 to 3600 cm^{-1}, indicating successful capping and hydrolysis of APTES.

As shown in Figure 3, the UV/Vis spectrum of $PNC_{APTES\text{-}2}$ exhibits an excitonic absorption peak at 521 nm, with a tail at longer wavelengths because of the scattering effect of large particles. With further addition of APTES, the PNC_{APTES} suspension showed less scattering and the absorption onset became blue-shifted, suggesting the formation of smaller PNCs. Similarly, a symmetric and narrow emission band with

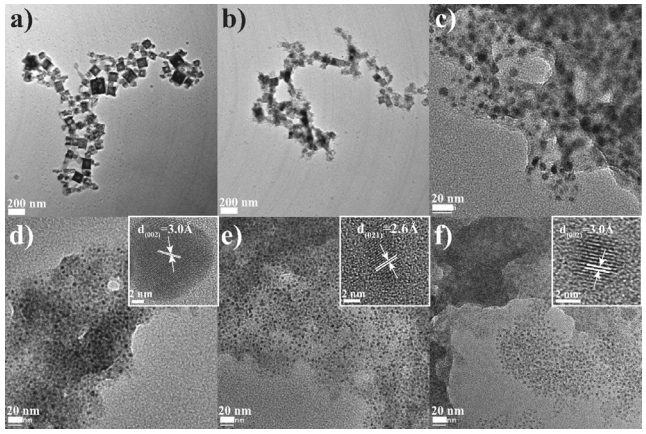

Figure 2. TEM images of PNCs prepared with different concentrations of APTES capping ligands. a) $PNC_{APTES\text{-}2}$, b) $PNC_{APTES\text{-}4}$, c) $PNC_{APTES\text{-}8}$, d) $PNC_{APTES\text{-}16}$, e) $PNC_{APTES\text{-}32}$, and f) $PNC_{APTES\text{-}64}$. Inset: HRTEM images of (d) $PNC_{APTES\text{-}16}$, (e) $PNC_{APTES\text{-}32}$, and (f) $PNC_{APTES\text{-}64}$.

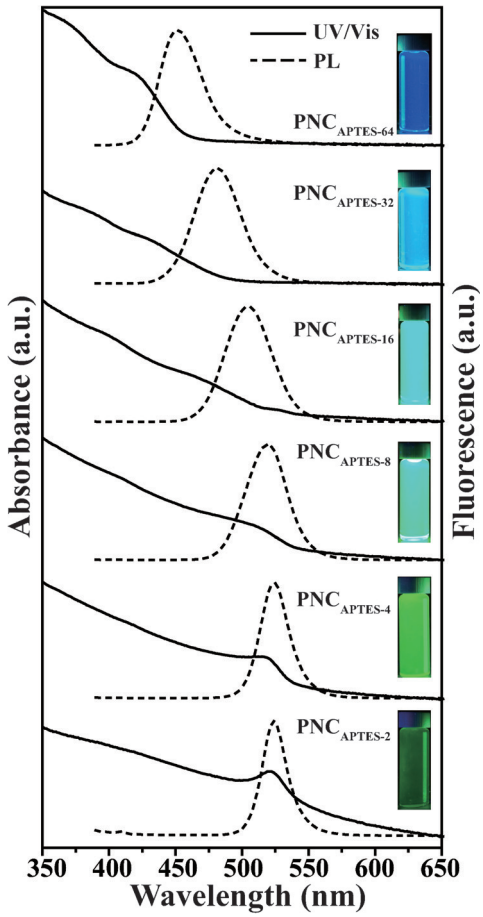

Figure 3. UV/Vis (solid line) and PL (dashed line) spectra ($\lambda_{ex} = 365$ nm) of PNC_{APTES} solutions prepared with different concentrations of APTES capping ligands. Inset: digital pictures of the PNC_{APTES} solutions under UV light.

a peak at 524 nm was observed for the 2 μL mL^{-1} APTES sample. However, an insufficient amount of ligands gave rise to poor passivation and low PL QY (ca. 2%). The highest PL QY (ca. 55%) was obtained with a slight emission shift when the APTES concentration was increased to 16 μL mL^{-1}. Although the emission could be further blue-shifted (Supporting Information, Table S1), the PL QY of PNC_{APTES} actually started to decrease. It is known that ligands coordinate to the surface atoms of NCs during the growth stage and create a stabilizing capping layer, which allows the delivery of monomers but prevents the agglomeration of as-formed NCs.[10] At high ligand concentration, the rate of monomer delivery through the ligand capping layer becomes slower because of the steric hindrance of ligands, resulting in smaller particles and more uncoordinated surface atoms, thereby lowering the PL QY. To demonstrate the generality of the APTES ligands, we also applied APTES in the synthesis of PNCs, including $CH_3NH_3PbCl_3$, $CH_3NH_3PbI_3$, $CH_3NH_3PbCl_{1.5}Br_{1.5}$, and $CH_3NH_3PbBr_{1.5}I_{1.5}$. Based on the PL spectra, all the samples show a size dependence on the amount of APTES (Supporting Information, Figure S3).

Compared to straight-chain ligands, branched ligands present substantial steric hindrance that favors the formation of smaller and more uniform NCs.[10] Cage-like POSS were previously applied in the controlled growth of layered perovskites.[11] Herein, NH_2-POSS was utilized as a capping ligand to further demonstrate size control with branched capping ligands beyond APTES (Supporting Information, Figure S4). Similar to the PNC_{APTES}, both the absorption and emission bands of $PNC_{NH2\text{-}POSS}$ were observed to blue-shift with an increasing concentration of NH_2-POSS. Furthermore, all $PNC_{NH2\text{-}POSS}$ solutions showed good dispersibility and high PL QY.

To date, several studies have employed the dissolution–precipitation strategy to fabricate high PL QY PNCs.[2b,e,6,9b] However, the PNCs capped by OA capping ligands tend to agglomerate into large particles with a low PL QY (< 10%) during precipitation (Supporting Information, Figure S5a). To achieve high PL QY, the large particles are often discarded and only the supernatant is kept after centrifugation, resulting in a low product yield.[2b,6] Moreover, the main components included in PNC_{OA} supernatant are always a mixture of PNPs and PNSs.[2c] In contrast, no large particles were formed during the precipitation described herein, and the PNCs synthesized using APTES showed high uniformity. To understand the different capping effects of OA and APTES, the optical properties of PNC precipitate, supernatant, and solution were studied. As shown in Figure 4a, the absorption and PL spectra of PNC_{OA} precipitate exhibited the characteristics of bulk materials,[12] with an identical absorption and emission peak position (ca. 533 nm). Besides this prominent peak, other PL peaks were evident between 475 and 500 nm,

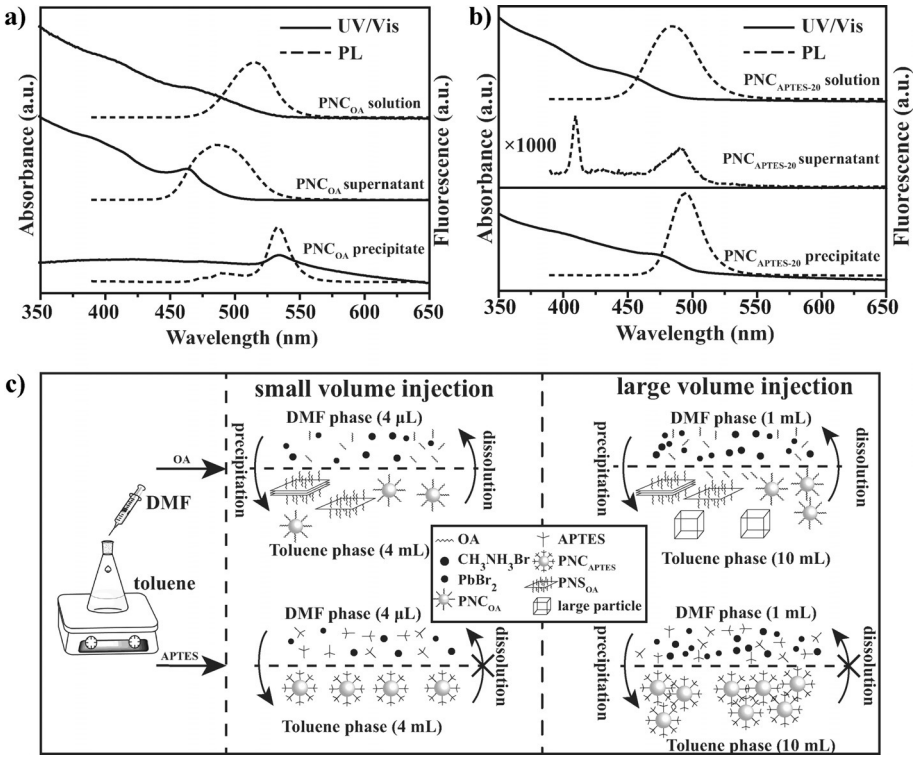

Figure 4. UV/Vis (solid line) and PL (dashed line) spectra (λ_{ex} = 365 nm) of a) PNC_{OA} and b) $PNC_{APTES\text{-}20}$ samples. c) Precipitation quantities influenced by OA and APTES ligand capping effects. The PL spectrum of PNC_{APTES} supernatant is magnified by 1000. The peak at 410 nm is likely to be a Raman signal from the solvent (Supporting Information, Figure S8).

owing to the presence of some PNSs.[9a,b] Compared to the low PL QY of PNC_{OA} precipitate (ca. 10%), the PNC_{OA} supernatant presented a broad emission band with a peak at approximately 488 nm with a high PL QY (ca. 60%), resulting from the various NCs with layer-dependent optical properties.[9a,b,13] Although the PNC_{OA} solution (QY: ca. 63%) also exhibited a single emission band centered at approximately 515 nm, the broad peak in the PL spectrum of PNC_{OA} solution suggests a non-uniform particle size. Note that the PL QY of PNC_{OA} solution is a little higher than that of PNC_{APTES} and $PNC_{NH2\text{-}POSS}$ because of the improved passivation of straight ligands, which results from weaker steric hindrance and repulsion of straight-chain ligands (Supporting Information, Figure S6).

The absorption and emission spectra collected for $PNC_{APTES\text{-}20}$ showed a very different pattern (Figure 4b). Significantly, the emission spectra of $PNC_{APTES\text{-}20}$ precipitate, supernatant, and solution all exhibit the PNC characteristic emission band with a peak at approximately 485 nm, showing that the size of the PNCs in these three systems is highly

uniform. The low absorption/emission intensity of $PNC_{APTES\text{-}20}$ supernatant is attributed to the low concentration of PNCs. This indicates that the as-formed PNCs can be easily collected by centrifugation (Supporting Information, Figure S5b), which is desirable for cleaning and post-processing in various applications.

To explain the different capping effects of OA and APTES, we propose the following mechanism based on a dissolution–precipitation model (Figure 4c). The dissolved precursors precipitate as PNCs at the DMF–toluene interface when the DMF precursor solution is injected into toluene. With OA as the capping ligand, the OA molecules adsorbed on the surface of the formed PNCs and PNSs diffuse from DMF to toluene, along with the products. However, the chain configuration of OA molecules cannot effectively prevent the products from dissolving back into DMF across the DMF–toluene interface and some OA ligands remain in the toluene phase because of their non-polar nature. The loss of OA ligands will result in a lack of ligands in the DMF phase, leading to the formation of large particles in the next round of precipitation. This effect becomes more pronounced when the concentrations of the precursors is high. On the contrary, the strong steric hindrance of APTES and the formation of silica can prohibit the dissolution of the as-formed PNCs back into DMF, which helps to maintain the original structural and optical properties of PNCs. Nevertheless, the $PNC_{APTES\text{-}20}$ sample began to flocculate after standing for a few minutes (Supporting Information, Figure S7) because of hydrolysis of Si-*O*-C_2H_5 groups attached to the PNC_{APTES} surface, which generate hydroxy (-OH) groups (as indicated by FTIR spectra), resulting in a change in polarity and hydrogen bonding of the ligands.

Water-induced degradation is a major problem for organic metal halide perovskites because protons are captured by methylammonium.[8] Similarly, they are also unstable towards other protic solvents such as alcohols.

We hypothesized that PNC_{APTES} may exhibit better stability because of the strong steric hindrance and hydrolysis properties of APTES, which reduces the access of protic solvent molecules to the PNCs surface. To test the stability of PNC_{APTES} in protic solvents, 0.5 mg mL^{-1} of PNC precipitate capped by different ligands was dispersed in ethanol (Supporting Information, Figure S9a and b). No emission was observed by the naked eye for PNC_{OA} and PNC_{OABr} dispersed in ethanol, and all XRD peaks (Supporting Information, Figure S9c) of the decomposed products belong to rhombic $PbBr_2$ (JCPDS#31-0679). However, the PNC_{APTES} precipitate showed high fluorescence intensity after sonication in ethanol, indicating better stability of PNC_{APTES} in protic solvents.

Long term stability tests were also conducted in different protic and polar solvents. As shown in Figure 5a, the relative PL intensity of the $PNC_{APTES\text{-}16}$ precipitate in isopropanol remained almost 70% after 2.5 h. However, $PNC_{APTES\text{-}16}$ precipitate showed poorer stability when dispersed in methanol and ethanol, which could be due to the smaller size of solvent molecules, which would allow easier passage through the ligand layer to the PNC surface. This was also true for the $PNC_{APTES\text{-}4}$ and $PNC_{APTES\text{-}8}$ precipitates of larger

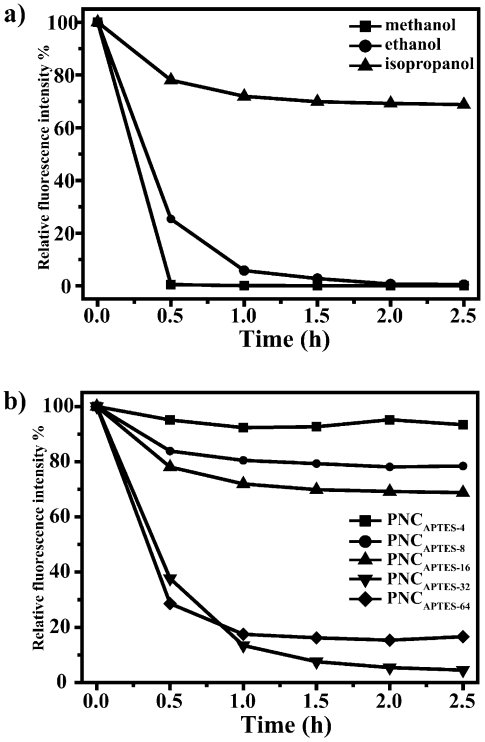

Figure 5. a) The relative fluorescence intensity of 0.5 mg mL^{-1} $PNC_{APTES\text{-}16}$ precipitate as a function of time in different protic solvents. b) The relative fluorescence intensity of PNC_{APTES} precipitate as a function of time in isopropanol.

particle size (Supporting Information, Figure S10). The stability of varying sizes of PNC_{APTES} precipitates in isopropanol was also studied. As shown in Figure 5b, stability improved for particles larger than $PNC_{APTES\text{-}16}$, but declined for smaller particles, possibly because of poorer surface passivation and an increase in surface defects.

In conclusion, branched capping ligands (APTES and NH_2-POSS) were successfully applied to the synthesis of PNCs, resulting in materials with improved stability. By controlling the amount of ligand present, uniform PNCs with tunable size (ca. 2.5–100 nm) and high PL QY (ca. 15–55%) were obtained. Compared to straight-chain ligands, OA and OABr, APTES and NH_2-POSS offer greater control over particle size and uniformity, which is attributed to their strong steric hindrance and the extent to which they protect PNCs from dissolution by DMF. A possible mechanism based on dissolution–precipitation processes was proposed to explain the role of different capping effects in controlling the uniformity of PNC size. Importantly, PNC_{APTES} shows improved stability in protic solvents compared to PNCs capped by straight OA or OABr ligands, which is attributed to strong steric hindrance and hydrolysis properties of APTES. The results demonstrate that the stability of PNCs can be substantially improved using branch-structured capping ligands, which is important for many emerging applications that utilize PNCs.

Acknowledgements

This project was supported by NASA (MACES Center), the BES division of the U.S. DOE, and UCSC Senate Special Research Fund. Work at the Molecular Foundry was supported by the Office of Science, Office of Basic Energy Sciences, the U.S. Department of Energy under Contract No. DE-AC02-05CH11231. B.L. is thankful for financial support from the China Scholarship Council (CSC). Y.-C.P. acknowledges financial support from the Ministry of Science and Technology, Taiwan R.O.C. (MOST-104-2113-M-024 -002-MY2). We thank Yi Peng for helpful discussions and Tianyu Liu for help on improving the writing.

Keywords: (3-aminopropyl)triethoxysilane (APTES) · nanocrystals · nanocrystal stability · organolead halide perovskites · photoluminescence

How to cite: *Angew. Chem. Int. Ed.* **2016**, *55*, 8864–8868
Angew. Chem. **2016**, *128*, 9010–9014

[1] a) N. K. Noel, A. Abate, S. D. Stranks, E. S. Parrott, V. M. Burlakov, A. Goriely, H. J. Snaith, *ACS Nano* **2014**, *8*, 9815–9821; b) F. Zhang, W. Ma, H. Guo, Y. Zhao, X. Shan, K. Jin, H. Tian, Q. Zhao, D. Yu, X. Lu, G. Lu, S. Meng, *Chem. Mater.* **2016**, *28*, 802–812; c) K. Aitola, K. Sveinbjörnsson, J.-P. Correa-Baena, A. Kaskela, A. Abate, Y. Tian, E. M. J. Johansson, M. Grätzel, E. I. Kauppinen, A. Hagfeldt, G. Boschloo, *Energy Environ. Sci.* **2016**, *9*, 461–466; d) Y. Li, Y. Zhao, Q. Chen, Y. M. Yang, Y. Liu, Z. Hong, Z. Liu, Y. T. Hsieh, L. Meng, Y. Li, Y. Yang, *J. Am. Chem. Soc.* **2015**, *137*, 15540–15547; e) Y. Yang, W. Wang, *J. Power Sources* **2015**, *293*, 577–584; f) A. Abate, M. Saliba, D. J. Hollman, S. D. Stranks, K. Wojciechowski, R. Avolio, G. Grancini, A. Petrozza, H. J. Snaith, *Nano Lett.* **2014**, *14*, 3247–3254.

[2] a) H. Huang, F. Zhao, L. Liu, F. Zhang, X. G. Wu, L. Shi, B. Zou, Q. Pei, H. Zhong, *ACS Appl. Mater. Interfaces* **2015**, *7*, 28128–28133; b) F. Zhang, H. Zhong, C. Chen, X. Wu, X. Hu, X. Huang, J. Han, B. Zou, Y. Dong, *ACS Nano* **2015**, *9*, 4533–4542; c) Y. Ling, Z. Yuan, Y. Tian, X. Wang, J. C. Wang, Y. Xin, K. Hanson, B. Ma, H. Gao, *Adv. Mater.* **2016**, *28*, 305–311; d) A. Swarnkar, R. Chulliyil, V. K. Ravi, M. Irfanullah, A. Chowdhury, A. Nag, *Angew. Chem. Int. Ed.* **2015**, *54*, 15424–15428; *Angew. Chem.* **2015**, *127*, 15644–15648; e) S. Pathak, N. Sakai, F. W. R Rivarola, S. D. Stranks, J. Liu, G. E. Eperon, C. Ducati, K. Wojciechowski, J. T. Griffiths, A. A. Haghighirad, A. Pellaroque, R. H. Friend, H. J. Snaith, *Chem. Mater.* **2015**, *27*, 8066–8075; f) A. B. Wong, M. Lai, S. W. Eaton, Y. Yu, E. Lin, L. Dou, A. Fu, P. Yang, *Nano Lett.* **2015**, *15*, 5519–5524; g) X. Zhang, H. Lin, H. Huang, C. Reckmeier, Y. Zhang, W. C. Choy, A. L. Rogach, *Nano Lett.* **2016**, *16*, 1415–1420.

[3] S. Zhuo, J. Zhang, Y. Shi, Y. Huang, B. Zhang, *Angew. Chem. Int. Ed.* **2015**, *54*, 5693–5696; *Angew. Chem.* **2015**, *127*, 5785–5788.

[4] a) Y. Wang, X. Li, J. Song, L. Xiao, H. Zeng, H. Sun, *Adv. Mater.* **2015**, *27*, 7101–7108; b) G. Xing, N. Mathews, S. S. Lim, N. Yantara, X. Liu, D. Sabba, M. Gratzel, S. Mhaisalkar, T. C. Sum, *Nat. Mater.* **2014**, *13*, 476–480; c) H. Zhu, Y. Fu, F. Meng, X. Wu, Z. Gong, Q. Ding, M. V. Gustafsson, M. T. Trinh, S. Jin, X. Y. Zhu, *Nat. Mater.* **2015**, *14*, 636–642.

[5] a) L. C. Schmidt, A. Pertegas, S. Gonzalez-Carrero, O. Malinkiewicz, S. Agouram, G. Minguez Espallargas, H. J. Bolink, R. E. Galian, J. Perez-Prieto, *J. Am. Chem. Soc.* **2014**, *136*, 850–853; b) G. Niu, X. Guo, L. Wang, *J. Mater. Chem. A* **2015**, *3*, 8970–8980; c) J. M. Frost, K. T. Butler, F. Brivio, C. H. Hendon, M. van Schilfgaarde, A. Walsh, *Nano Lett.* **2014**, *14*, 2584–2590.

[6] H. Huang, A. S. Susha, S. V. Kershaw, T. F. Hung, A. L. Rogach, *Adv. Sci.* **2015**, *2*, 1500194.

[7] a) G. Morello, M. De Giorgi, S. Kudera, L. Manna, R. Cingolani, M. Anni, *J. Phys. Chem. C* **2007**, *111*, 5846–5849; b) S. D. Stranks, V. M. Burlakov, T. Leijtens, J. M. Ball, A. Goriely, H. J. Snaith, *Phys. Rev. Appl.* **2014**, *2*, 034007; c) J. Bang, Z. Wang, F. Gao, S. Meng, S. B. Zhang, *Phys. Rev. B* **2013**, *87*, 205131.

[8] E. Mosconi, J. M. Azpiroz, F. De Angelis, *Chem. Mater.* **2015**, *27*, 4885–4892.

[9] a) P. Tyagi, S. M. Arveson, W. A. Tisdale, *J. Phys. Chem. Lett.* **2015**, *6*, 1911–1916; b) J. A. Sichert, Y. Tong, N. Mutz, M. Vollmer, S. Fischer, K. Z. Milowska, R. Garcia Cortadella, B. Nickel, C. Cardenas-Daw, J. K. Stolarczyk, A. S. Urban, J. Feldmann, *Nano Lett.* **2015**, *15*, 6521–6527; c) B. Luo, Y.-C. Pu, Y. Yang, S. A. Lindley, G. Abdelmageed, H. Ashry, Y. Li, X. Li, J. Z. Zhang, *J. Phys. Chem. C* **2015**, *119*, 26672–26682.

[10] T. Morris, T. Zubkov, *Colloids Surf. A* **2014**, *443*, 439–449.

[11] S. Kataoka, S. Banerjee, A. Kawai, Y. Kamimura, J. C. Choi, T. Kodaira, K. Sato, A. Endo, *J. Am. Chem. Soc.* **2015**, *137*, 4158–4163.

[12] a) Z.-K. Tan, R. S. Moghaddam, M. L. Lai, P. Docampo, R. Higler, F. Deschler, M. Price, A. Sadhanala, L. M. Pazos, D. Credgington, F. Hanusch, T. Bein, H. J. Snaith, R. H. Friend, *Nat. Nanotechnol.* **2014**, *9*, 687–692; b) G. Li, Z. K. Tan, D. Di, M. L. Lai, L. Jiang, J. H. Lim, R. H. Friend, N. C. Greenham, *Nano Lett.* **2015**, *15*, 2640–2644.

[13] G. C. Papavassiliou, I. R. Koutselas, *Synth. Met.* **1995**, *71*, 1713–1714.

Received: March 6, 2016
Revised: April 20, 2016
Published online: June 13, 2016

